Title
Climate effect of black carbon aerosol in a Tibetan Plateau glacier

Authors
Yang, Song
Xu, Baiqing
Cao, Junji
et al.

Publication Date
2015-06-01

DOI
10.1016/j.atmosenv.2015.03.016

Atmospheric Environment 111 (2015) 71–78

Contents lists available at ScienceDirect

Atmospheric Environment

journal homepage: www.elsevier.com/locate/atmosenv

Climate effect of black carbon aerosol in a Tibetan Plateau glacier

Song Yang [a, *], Baiqing Xu [a], Junji Cao [b], Charles S. Zender [c], Mo Wang [a]

[a] Key Laboratory of Tibetan Environment Changes and Land Surface Processes, Institute of Tibetan Plateau Research, Chinese Academy of Sciences, Beijing 100101, China
[b] Key Laboratory of Aerosol Science & Technology, SKLLQG, Institute of Earth Environment, Chinese Academy of Sciences, Xi'an 710075, China
[c] Department of Earth System Science, University of California, Irvine, CA 92697-3100, USA

HIGHLIGHTS

- We sampled surface snow and snow pits in the snowmelt season in a Tibetan glacier.
- We depicted the variability of BC, OC, and dust concentrations.
- Scavenging efficiency and enrichment for BC and OC were derived.
- We evaluated BC radiative forcing in snow using SNICAR.

ARTICLE INFO

Article history:
Received 28 August 2014
Received in revised form
6 March 2015
Accepted 9 March 2015
Available online 3 April 2015

Keywords:
Black carbon
Snow
Glacier melt
Tibetan Plateau

ABSTRACT

In the Tibetan Plateau, the black carbon (BC) concentration in surface snow and snow pits has received much attention, whereas the seasonal behavior of aerosol-in-snow concentration, vertical profile, melt-scavenging, and enrichment have received relatively little attention. Here we investigate these processes and their impacts on radiative forcing on the Muji glacier in the westernmost Tibetan Plateau during the 2012 snowmelt season. Increasing impurity concentrations were mostly due to post-deposition effects rather than new deposition. On 5 July, BC concentrations in the surface snow were higher than those of fresh snow, implying enrichment via sublimation and/or melting of previous snow. Fresh snow contained 25 ng g^{-1} BC on 27 July; afterward, BC gradually increased, reaching 730.6 ng g^{-1} in September. BC, organic carbon (OC), and dust concentrations co-varied but differed in magnitude. Melt-scavenging efficiencies were estimated at 0.19 ± 0.05 and 0.04 ± 0.01 for OC and BC, respectively, and the BC in surface snow increased by 20–25 times depending on melt intensity. BC-in-snow radiative forcing (RF) was approximately 2.2 W m^{-2} for fresh snow and 18.1–20.4 W m^{-2} for aged snow, and was sometimes reduced by the presence of dust.

1. Introduction

Black carbon (BC) deposited in snow absorbs more sunlight than pure snow due to significant differences between the optical properties of BC and ice (Bond and Bergstrom, 2006; Warren and Brandt, 2008). Slight initial changes in snow albedo due to BC, in conjunction with the rapid adjustments and feedbacks that ensue, can cause significant climate effects (Bond et al., 2013). The local radiative forcing (RF) may reach 4–25 W m^{-2} during spring in the Tibetan Plateau (TP) snowpack (Bond et al., 2013; Flanner and Zender, 2005; Flanner et al., 2007). Increased net radiation fosters earlier snow and glacier melt (Qian et al., 2011). As a result, BC may play an important role (Xu et al., 2009a) in the rapid retreat of TP glaciers (Yao et al., 2012). The complex terrain of TP, spatio-temporal heterogeneity of BC, and difficulty in remotely sensing (Warren, 2013) and modeling BC (Flanner et al., 2009) show that in situ observations are required for accurate estimates of BC concentration, behavior, effects on snowpack energy budgets and climate.

Numerous studies have focused on TP BC recorded in ice cores and in surface snow and snow pits (Kaspari et al., 2011; Ming et al., 2008; Wang et al., 2014; Xu et al., 2009a, 2009b). Few studies have characterized seasonal BC evolution in surface snow (Kaspari et al., 2014; Ming et al., 2009; Xu et al., 2006). Much of our knowledge of the behavior and effects of BC enrichment via melt and sublimation in snowpacks comes from earlier studies with limited snow

* Corresponding author.
E-mail address: yangsong@itpcas.ac.cn (S. Yang).

http://dx.doi.org/10.1016/j.atmosenv.2015.03.016
1352-2310/

stratigraphy and sites. Conway et al. (1996) conducted an experiment on Snowdome on the Blue glacier in the Olympic Range, USA and found that hydrophilic BC was more likely flushed by meltwater than hydrophobic BC. Both types had a scavenging efficiency <100%, implying residual BC in the surface snow. Based on these results, scavenging factors for two types of BC (3%, 20%) were estimated and used in CLM (Flanner et al., 2007; Oleson et al., 2013).

More recent snow sampling has improved our understanding of the variability of BC concentrations. Xu et al. (2006, 2012) sampled snow in the TP and Tienshan. During summer, both BC and OC concentrations increased by up to two orders of magnitude over those of fresh snow. Xu et al. (2009a) studied the spatio-temporal variation of calculated BC in a southeast TP glacier and found that BC could strongly impact snow albedo in the melt season. Ming et al. (2009) concluded that BC in snow showed a weak negative relationship with the sampling site elevation. Huang et al. (2011) showed BC-in-snow concentrations decrease rapidly towards the northeast and away from major industrial regions. In the Arctic, Doherty et al. (2010) and Forsstrom et al. (2013) showed that the spatial differences in BC depended on the emission source intensity, the distance from the source to the deposition region, and the prevailing wind direction. In the eastern Sierra Nevada, Sterle et al. (2013) noted that BC concentrations in aged snow were enhanced seven-fold relative to those in fresh snow. These studies depict BC-in-snow as highly variable with an estimated melt-scavenging efficiency of 10–30% (Doherty et al., 2013).

Data in the vast TP is insufficient to fully characterize BC variation in snow, its RF, or impacts on snow energy balance. Our study (1) depicts the spatio-temporal and vertical variability of BC and other light-absorbing materials, (2) derives the melt-scavenging and enrichment of OC and BC, and (3) estimates the BC RF in snow in the westernmost TP during the 2012 snowmelt season.

2. Samples and methods

Muji glacier (39.19 °N, 73.74 °E), which is ~20 km northeast of Lake Karakul, westernmost TP and under the control of the prevailing westerly jet stream (Xu et al., 2009a), has dry-cold climate with mean annual precipitation 76.3 mm and temperature −3.8 °C (Fig. 1) (Williams and Konovalov, 2008). During the 2012 snowmelt season, we staked the glacier (13 stakes, Fig. 1). The top ~8–10 cm of snow was sampled. Snow pits were also excavated, and samples were collected downward at 10 cm intervals at elevations of 5460 m and 4910 m.

Samples were melted at room temperature in a clean laboratory. Immediately after melt, the liquid was sonicated and filtered through quartz fiber filters (Supplemental Materials) (Schwarz et al., 2012; Wang et al., 2012). BC and OC on the filters were measured using a method similar to the IMPROVE protocol (Cao et al., 2003; Chow et al., 2004). Because the filters had more dust load than those collected from ice core samples or aerosol samples (Wang et al., 2012), we modified the method that in 100% helium atmosphere, only a temperature plateau (550 °C) was arranged to reduce the time that BC was exposed in catalyzing atmosphere. BC results were reported regardless of the optical signal. To identify uncertainty stemming from instrumental instability and uneven distribution of carbon particles in filters, duplicates of ~40% of samples were analyzed separately, with consistent results ($R^2 = 0.979$).

The stratigraphy of other snow properties was also investigated. The presence of dust was monitored by drying the quartz fiber filters and weighting the mass on them (Kaspari et al., 2014; Painter et al., 2012). Snow density was measured with a stainless steel tube-type cutter and a scale (Conger and McClung, 2009).

We evaluated the daily mean BC RF in the snowpack using the SNICAR model (Flanner et al., 2007; Toon et al., 1989; Wiscombe and Warren, 1980), which has 470 solar bands, constrained by the BC and dust concentrations in surface snow. We estimated the clear-sky and cloudy spectral flux with a 30-min time step, using the SBDART model (Ricchiazzi et al., 1998; Stamnes et al., 1988). Calculations were done for clear-sky and cloudy conditions with a 30-min time step and weighted equally to obtain BC RF in snow (Eq. (1), (2)) (Kaspari et al., 2014; Sterle et al., 2013):

$$RF = \sum_{0.305\mu m}^{4.995\mu m} E(\lambda,\theta)\left(\alpha_{(r,\lambda)} - \alpha_{(r,\lambda,imp)}\right)\Delta\lambda \quad (1)$$

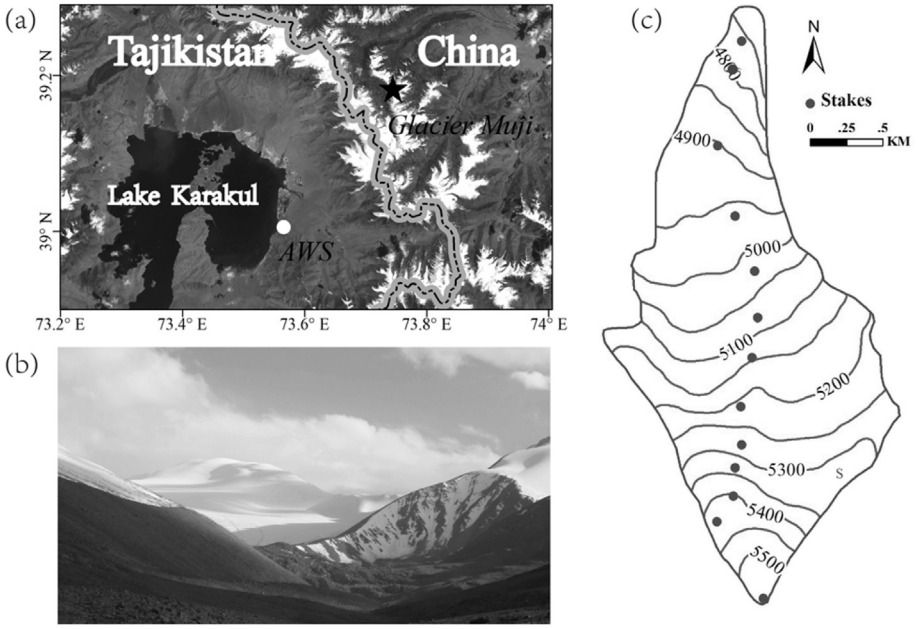

Fig. 1. (a) Muji glacier and Lake Karakul (circle: AWS, star: glacier); (b) Muji glacier close-up; and (c) Topography (m) of Muji glacier with the distribution of stakes.

$$RF_{day} = 1/2 \times \sum_{0h}^{24h} (RF_{clr} + RF_{cld})\Delta t \Big/ \sum_{0h}^{24h} \Delta t \quad (2)$$

where RF and RF_{clr}, RF_{cld}, RF_{day} represent the instantaneous RF, RF in clear sky, RF in cloudy sky and daily mean RF, respectively; α is the modeled snow spectral albedo with/without the impurities (imp) of BC and/or dust, E is the spectral irradiance, r is the snow optical grain size, λ is wavelength (μm), and θ is the solar zenith angle (Michalsky, 1988). The optical properties of aerosols and snow were from SNICAR and BC was assumed to be coated with sulfate (Flanner et al., 2007).

3. Results and discussions

3.1. Deposition variability of BC, OC and dust

Back trajectories (Fig. 2) reveal that during the sampling period the air parcels typically passed over Afghanistan, Pakistan, central Asia, and western China as noted during previous studies for the same region (Cao et al., 2009).

Although the prevailing winds over the study region are westerlies, ice core and atmospheric aerosol studies in the Muztagh Ata region show that BC, OC and dust concentrations peak in summer (seasonal BC in unpublished data; Cao et al., 2009; Wu et al., 2008), rather than in winter as in other TP regions (Kaspari et al., 2014; Xu et al., 2009a). The BC and OC summer peak could be due to agricultural burning and wildfires in the dry and hot source regions (Giglio et al., 2006). The summer climate also makes soil conditions more favorable for dust storm formation in some dust source regions, contributing a high dust load in summer in Muztagata ice cores (Wu et al., 2008). The Muji Glacier is far from known emission sources, so we assume that BC/OC/dust deposition is homogeneous in our small study area. However, measured concentrations in aged snow are far higher than those in fresh snow and the variability exceeds the seasonality of deposition. This implies that processes other than dry and wet deposition play a crucial role. The likeliest process responsible for enriching the concentration of insoluble snowpack impurities in surface snow is that the impurities not flushed away in meltwater remain behind in the unmelted snow (Doherty et al., 2013; Sterle et al., 2013; Xu et al., 2012).

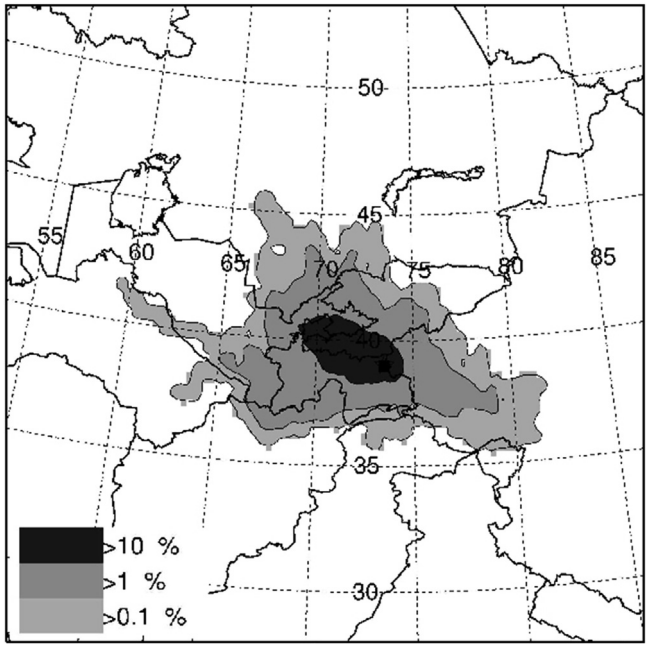

Fig. 2. 48 h air mass back-trajectory frequency during the investigated period spanning from July to September, 2012 (at 500 m height above ground) computed by the HYSPLIT model (http://ready.arl.noaa.gov/HYSPLIT.php) using NCEP reanalysis data.

3.2. Spatio-temporal variability in surface snow BC

In surface snow BC concentrations were assumed constant at the measured elevations and then linearly extrapolated over the entire glacier area. The glacier-mean surface snow aerosol concentrations varied significantly with time and elevation (Fig. 3, Fig. 4).

On 5 July, only two surface snow samples were collected, containing 73.9 ng g^{-1} and 41.1 ng g^{-1} BC. These relatively high values could be due to previous sublimation or melt (Doherty et al., 2010). On 10 July, much higher BC concentrations were consistent with rapid BC enrichment once the snow began to melt. Fresh snowfall at 1.2 mm w.e./day followed by mixing with old surface snow may explain the low BC concentrations in the next two collections. Snowfall at 2.3 mm w.e./day occurred before 27 July. This covered the whole glacier resulting in the lowest recorded BC concentration of 25 ± 10.3 ng g^{-1}, a value we considered a benchmark for fresh snow on this glacier. Snow fell again in early August, when BC measurements were comparable to those on 27 July. Despite the snowfall in mid- and late August, the ongoing melt gradually enriched BC faster than fresh snow diluted it, resulting in net BC increases. In September, snowmelt weakened, but the BC continued to rise. The greatest measured BC on the glacier was 730.6 ± 167.2 ng g^{-1} on 15 September. Six fresh snow samples were collected on 25 October, when it was difficult to detect snowmelt. By then BC had returned to its initial level of early July, and dirty snow was buried by fresh snow. Even though no more data were taken afterwards, we could speculate that the BC in surface snow depended only on deposition and

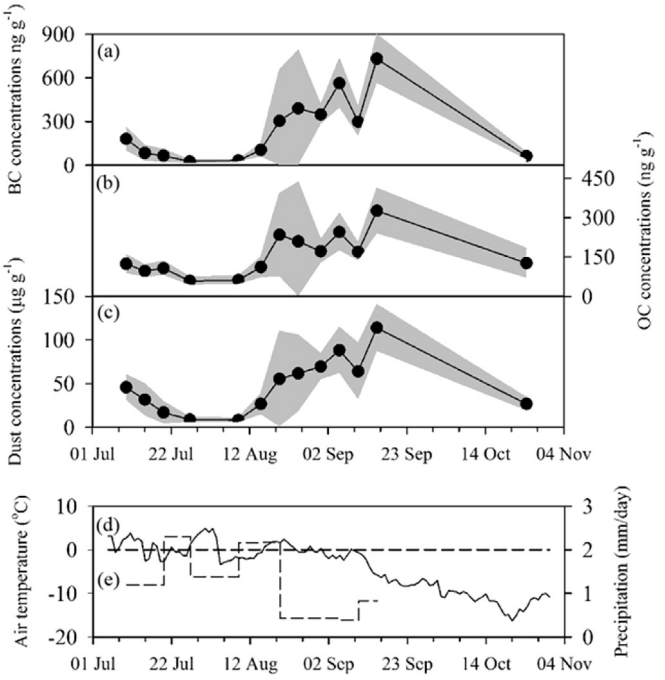

Fig. 3. Mean BC (a), OC (b), and dust (c) concentration in the surface snow averaged for the glacier grids; shading indicates ±1 standard deviation from the mean. Air temperature (d) recorded by the sensor at an elevation of 4910 m and daily precipitation (e) averaged from records of three rain gauges in the glacier and surroundings (at elevations of 5460 m, 5340 m, and 4700 m).

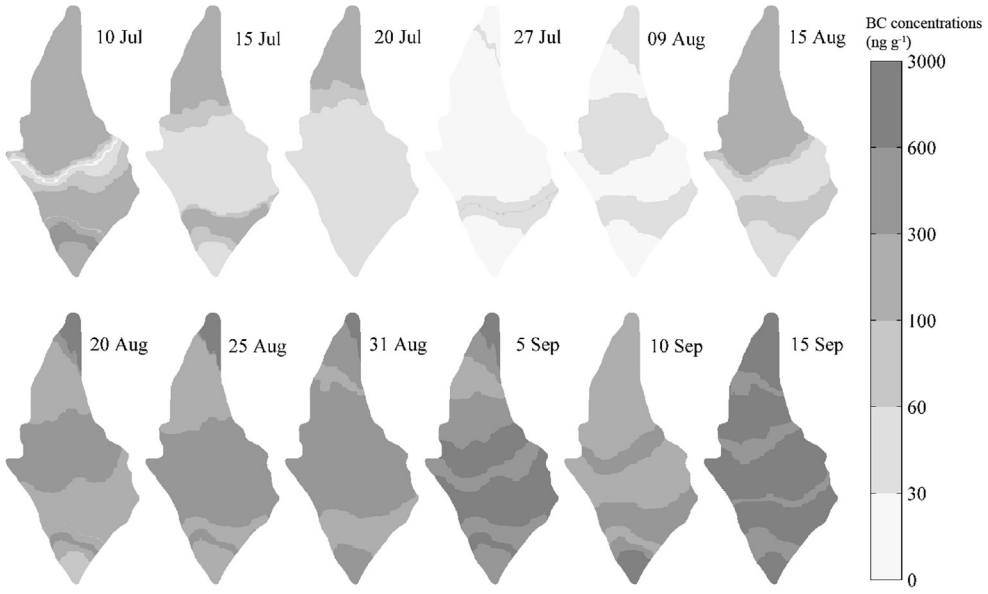

Fig. 4. Measured BC in the surface snow (5 July and 25 October were excluded due to limited available samples).

sublimation until the next melt season in spring 2013.

At different sites during our survey, BC enrichment can be explained by the difference in snowmelt strength among the sites. In other words, more intense melt exposed more BC to the surface at lower elevations (and warmer temperatures). This phenomenon was evident in late August when BC gradients were strong, whereas gradients were relatively weak in July and September when fresh snow fell and snow underwent significant melt, respectively.

Other impurities variations were consistent with BC throughout the investigations, differing mainly in magnitude (Fig. 3). The smallest and largest concentrations for OC were 58.4 ± 15.6 ng g^{-1} and 325.8 ± 86.5 ng g^{-1} on 27 July and 15 September, respectively, whereas those for dust were 8.9 ± 2.3 μg g^{-1} and 113.8 ± 26.7 μg g^{-1}. In light of the similar behavior of dust, OC and BC, the separate analysis of dust is omitted from the subsequent text.

3.3. Vertical variability of OC and BC

We primarily discuss the higher elevation profiles where snow layers were thicker and more robust (Fig. 5). OC and BC profiles showed wide variation across snow pits, ranging from 29.7 to 297.3 ng g^{-1} for OC and from 12.5 to 733.7 ng g^{-1} for BC, and these extreme values all appeared at the snow pit acquired on 10 September. Maximum OC and BC concentrations frequently occurred at the snowpack top, except after fresh snow. Minimum OC and BC concentrations usually occurred in fresh snow and buried old snow samples that experienced flushing from above. Fresh snow buried old snow and immediately beneath this pure surface, OC and BC were more abundant than in the adjacent fresh snow above and old snow below.

The vertical distributions of OC and BC concentrations collected on 5 July were uniform, indicating that OC and BC were not enriched in the surface snow, nor had they migrated downward. OC/BC ratios (Fig. 6) were approximately those of fresh snow (~2) and consistent with insignificant snowmelt prior to 5 July. Enriched OC and BC generally occurred at depths 0–40 cm, except after fresh snow reduced impurities in the top layer as in late July. Below 40 cm, impurities were initially unenriched, but as the melt season progressed, BC scavenged from upper snow layers flushed downwards and accumulated here (Xu et al., 2012). The greatest bottom firn BC measured was 137 ng g^{-1} on 15 September. Melt water scavenged OC more efficiently than BC, although more constrained experiments are necessary to confirm this. Impurity concentrations in the bottom firn held steady for all samples, except for the high BC values on 15 September.

The lower elevation (4910 m) snow pit (Fig. 5) tells a different story, although only a few samples are available. The snowpack had already experienced dramatic melt, and only a 46-cm depth of snow remained when we first sampled on 10 July. After 15 August no subsurface samples were available. On 10 July, the highest OC and BC concentrations and lowest OC/BC ratio (0.5) indicated that the OC and BC had redistributed vertically primarily under the control of strong meltwater. Afterwards, the variations were consistent with the 5460 m profiles.

The scavenging efficiency for impurities via snow meltwater is defined as the ratio of the concentration in the meltwater flux that leaves a snow layer relative to the bulk concentration in that snow layer (Flanner et al., 2007). We determined the scavenging efficiency using the model of Doherty et al. (2013). The samples collected on 27 July and 15 September were identified as no melt and sufficient melt samples, respectively (Table 1).

The best estimates of scavenging efficiencies were 0.19 ± 0.05 for OC and 0.04 ± 0.01 for BC, respectively. Consistent with previous studies (Xu et al., 2012), OC was more hydrophilic than BC and dust, and more likely to wash downward through the snow with meltwater. Including uncertainties, our results were consistent with scavenging efficiencies of 0.03 for hydrophobic OC and BC and 0.2 for hydrophilic OC and BC (Flanner et al., 2007) and the BC scavenging efficiencies of 0.10–0.30 (Doherty et al., 2013).

Our fresh snow BC concentrations at Muji Glacier were 1.5-times greater than records from the last decade of the 20th century from the Muztagh Ata ice core (Xu et al., 2009a). Therefore, our calculated scavenging efficiency via melt water and enrichment analysis could be biased. Furthermore, scavenged impurities could be retained in the sampled subsurface snow (Conway et al., 1996), exaggerating the impurities considered non-scavenged, and lowering the estimated scavenging efficiency. Moreover, the assumption that the snow undergoes a sufficient concentration of melt (Doherty et al., 2013) was not always met, and thus, the

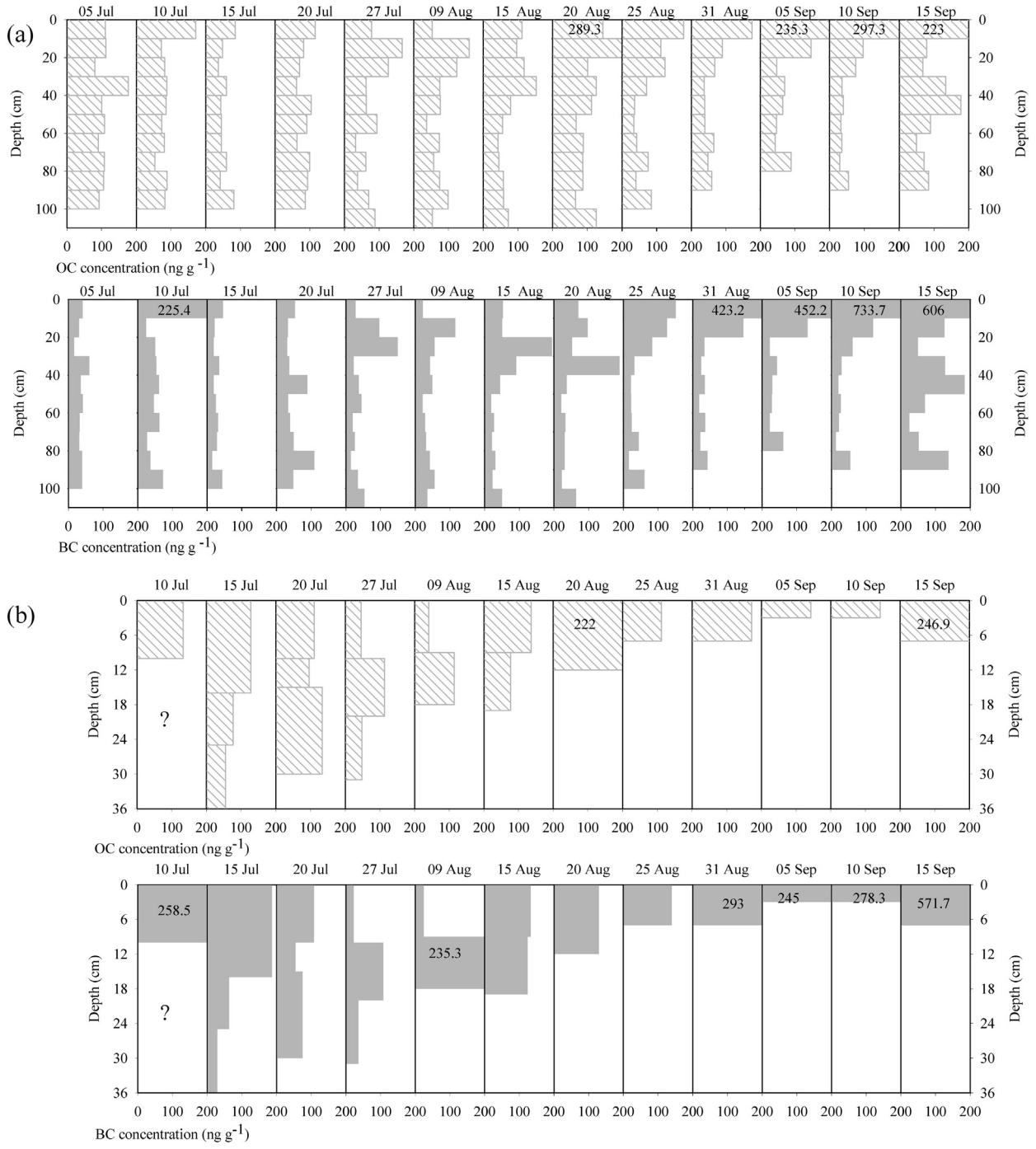

Fig. 5. OC and BC across snow pit profiles at elevations of 5460 m (a) and 4910 m (b).

calculated results could represent upper limits on scavenging. Other variables, i.e., specific surface area, water films, and precipitation, should impact the scavenging in snowpack. As suggested by Doherty et al. (2013), more and better constrained measurements are required in future.

Our measurements indicated that during surface melt events only a minute portion of the impurities were completely scavenged out of the snowpack; meltwater vertically redistributed the remainder which is retained and enriched concentrations deeper in the snowpack. The OC and BC in surface snow and in the bottom firn for each snow pit were extracted, and the values were divided by the corresponding concentrations for fresh snow. The results (defined herein as 'enrichment') are presented in Fig. 6. Also shown are the corresponding OC/BC ratios. Samples collected on 5 July are excluded from our analysis.

Enrichment varied with snow depth, impurity species, and elevation. The highest enrichments for BC in surface snow, found during the early fall, were ~25 and ~20 for the high and low snow pits, respectively. BC in surface snow for both snow pits increased gradually after 9 August, whereas OC plateaued with little fluctuation, implying that once melt rates reached a threshold (the subject in future work), new OC was offset by flushing. In the bottom of

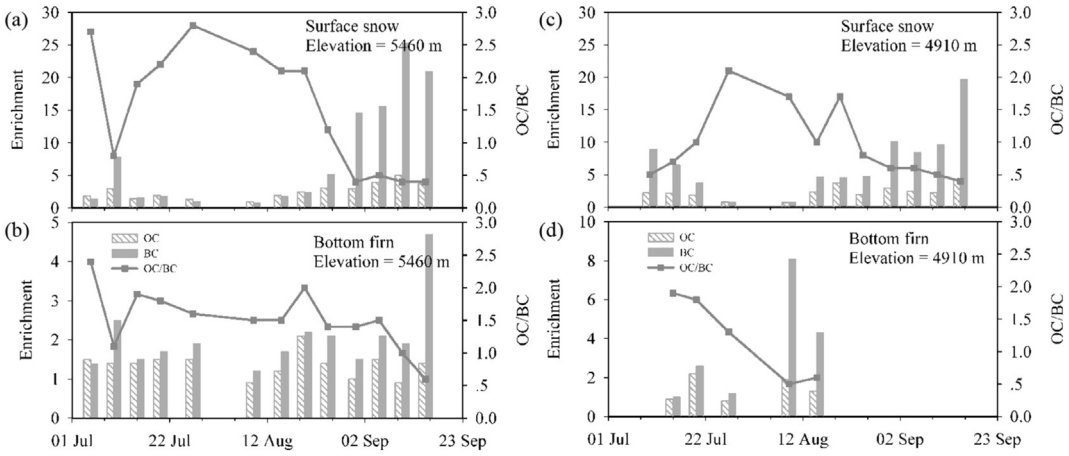

Fig. 6. Enrichment of BC and OC and the evolution of the OC/BC ratios in surface snow (a, c) and bottom firn (b, d) for two snow pits.

Table 1
Snow properties for deriving the scavenging efficiency.

Snow status	BC concentration (ng g^{-1})	OC concentration (ng g^{-1})
No melt	25 ± 10	58 ± 16
Sufficient melt	730 ± 167	326 ± 87

the higher snow pit, OC and BC enrichment did not vary until late August, when flushed OC and BC finally reached the bottom firn. BC enrichment peaked in mid-September once the BC reached the bottom firn.

OC/BC ratios were highest for surface fresh snow, reaching 2.3 on 27 July and 2.1 on 25 October. These were consistent with the ice core record of 2.2 in Muztag Ata (Xu et al., 2009a). The ratio gradually decreased to less than 1 during late August and the first half of September. The decreasing trend of OC/BC during snowmelt periods showed that snowmelt scavenges OC more efficiently than BC. OC/BC held steady at ~0.5 during the early fall, implying that OC and BC scavenging efficiency both remained constant.

3.4. Comparison of the results to other studies

Surface snow and snow pits profiles were also sampled in the TP and surroundings in previous studies. The minimum reported BC in surface snow was at the Mera Col, Himalaya (1.0 ng g^{-1}/18 ng g^{-1}) on Mt. Everest and at Haxilegen River No. 48 (11 ng g^{-1}) in the Tianshan range (Kaspari et al., 2014; Ming et al., 2009); . The maximum reported BC in surface snow was at the Meikuang glacier (446 ng g^{-1}) in the northeastern TP, at Urumqi glacier No. 1 (Urmq1) (~500 ng g^{-1}) in the Tianshan and at Mera La (1290 ng g^{-1}) (Kaspari et al., 2014; Xu et al., 2012, 2006). In addition, the maximum reported OC and BC in snow pits at the Zhadang glacier in the central TP was ~600 ng g^{-1} BC, and at Urmq1 was~8000, ~3000 ng g^{-1}. Here the dirtiest snow layer in the snow pit was 25–35 cm below the surface, well above the bottom of snow pit. Our samples fall in the envelope of these studies, except for those samples collected at the glacier terminus. Note that these studies are not directly intercomparable for all purposes due to different analysis methods (Torres et al., 2014), sampling dates, and snow

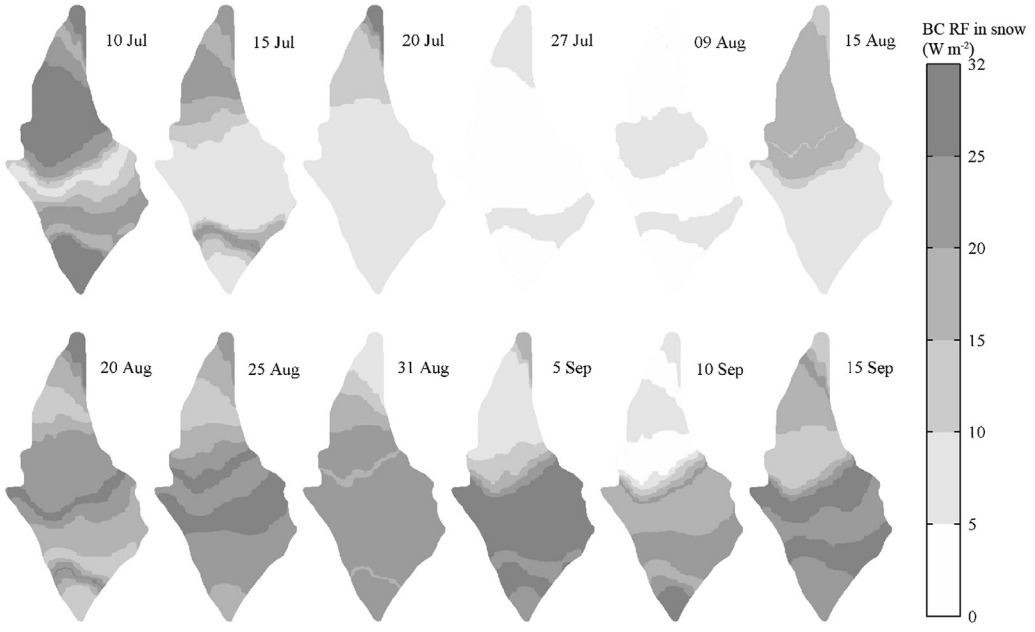

Fig. 7. BC RF in the snowpack with snow grain size 750 μm.

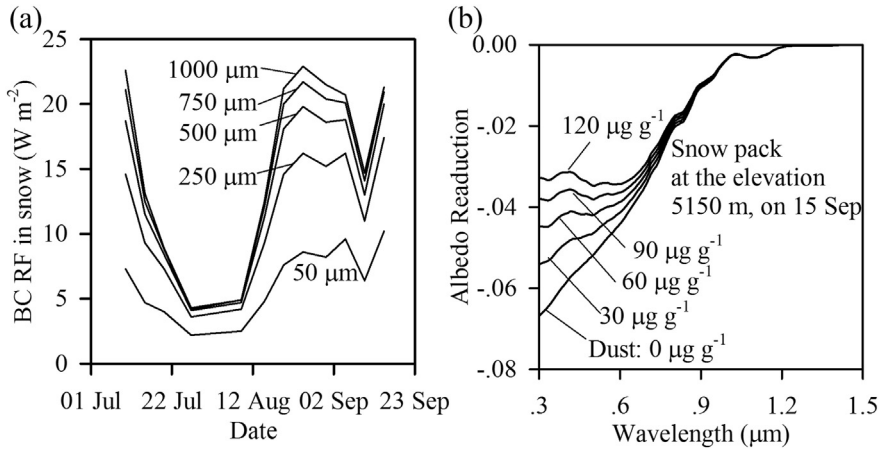

Fig. 8. BC RF in snow averaged for the glacier grids for different snow grain sizes (a), and snow albedo reduction due to BC for different dust contamination status (b).

aging, and thus the estimated efficiency of BC RF in snow is expected to vary (Kopacz et al., 2011; Lee et al., 2013).

3.5. BC RF in snow

We estimated BC RF with SNICAR (Flanner et al., 2007) considering a range of snow optical grain sizes: 50, 250, 500, 750, and 1000 μm. The minimum and maximum sizes corresponded to fresh snow and to well-aged, wet snow or grain clusters (Nolin and Dozier, 2000). Snow depth and density were as measured in the field observations. Estimated BC RFs for the 750 μm snow grain size are illustrated in Fig. 7 and Fig. 8.

The lowest BC RFs were noted on 27 July and 9 August after snowfall, and the largest values were found during the late summer when RF drastically increased (Figs. 7 and 8). Snow grain size changes dynamically due to metamorphic aging, and this influences both the snow albedo and the RF of snow impurities (Warren and Wiscombe, 1980; Wiscombe and Warren, 1980). As shown in Fig. 8, BC RF sensitivity to grain size was more obvious in the early fall when there was more BC. In the clean fresh snow, the variability of BC RF due to snow grain size was minimal. Cleary, accurate measurements of optically effective grain size are required to estimate the BC RF in snow. We measured the geometric (not optically effective) grain size using a hand lens. Although the results were somewhat subjective and not identical between observers, and not equivalent to optical grain size, the geometric size of aged and rounded snow is approximately the optical grain size. Measured grain size in the late summer ranged from 500 to 1000 μm, corresponding to BC RF of 18.1–20.4 W m^{-2} (Fig. 8). Lens-based methods have difficulty identifying grain size for complex shapes, so we assumed 50 μm for fresh snow (Nolin and Dozier, 2000). The resulting BC RF in late July was ~2.2 W m^{-2}. Though these assumptions are highly uncertain, the results yield a preliminary idea of BC RF in snow in the westernmost TP.

The presence of dust in snow may reduce BC RF, and the impact of BC may be negligible when dust concentrations are high (Kaspari et al., 2014). We extracted the stratigraphy at 5150 m on 15 September, employed actual BC and scaled dust in surface snow (0–120 μg g^{-1}, and its actual value 109.6 μg g^{-1}) to assess the influence of dust on the snow albedo reduction due to BC under the clear sky at noon (Fig. 8). At 0.305 μm, snow albedo reduction due to BC is 0.0666 without dust and 0.0328 for 120 μg g^{-1} dust. Minute dust (<10 μg g^{-1}) in fresh and clean snow slightly impacts BC RF in July and early August, while large amount of dust in aged snow significantly reduces BC RF in the early fall. BC in snow is regarded as the active factor controlling snow albedo and snow-ice RF (Bond et al., 2013), yet from our study, dust also play an important role with increasing concentration (Fig. 8), and the phenomenon is particularly evident when dust goes up to the extremely high level in the glacier terminus or in the early fall.

Numerous modeling studies of BC RF have been conducted in the TP and surroundings. Maximum BC RF occurs with the combination of high BC in snow, surface-incident solar flux, and snow cover. Previous studies found BC RF of up to 20 W m^{-2} over the TP during the spring (Qian et al., 2011). The RF in summer and autumn is generally lower due to snow loss (Flanner et al., 2009). However, the glaciers melt during summer and this enriches BC (Xu et al., 2012) and increases RF. Our estimated RF at Muji Glacier is higher than previous studies over the TP because of BC enrichment by melt-scavenging, except for the Nyainqentanglha (Ming et al., 2013).

4. Conclusions

We staked a glacier in the westernmost TP and sampled the surface snow and snow pits during the 2012 snowmelt season. Increasing impurities concentrations were mostly because of post-depositional processes including enrichment due to melt-scavenging. On 10 July, the average BC, OC, and dust concentrations in the surface snow were 179.4 ng g^{-1}, 123.4 ng g^{-1}, and 45.6 μg g^{-1}, respectively. Fresh snow contained much lower impurity concentrations, 25 ng g^{-1}, 58.4 ng g^{-1}, and 8.9 μg g^{-1} on 27 July. Old snow exposed to impurities throughout the summer, contained OC, BC and dust at 730.6 ng g^{-1}, 325.8 ng g^{-1}, and 113.8 μg g^{-1}on 15 September. During the study period, BC, OC and dust co-vary. BC changes at different sites were consistent with an elevation/temperature-dependent difference in snowmelt strength.

Impurity concentrations were highly variable across pits. The maxima frequently occurred in surface snow, and the minima usually occurred in fresh snow samples or old snow samples that had been flushed by meltwater from above. We estimate scavenging efficiencies of 0.19 ± 0.05 for OC and 0.04 ± 0.01 for BC. Snowmelt and/or sublimation enriched BC in surface snow by 20–25 times relative to fresh snow. The decreasing OC/BC ratio trends with depth showed that melt water scavenges OC more efficiently than BC.

Snowpack radiative forcing (net absorption) by BC was ~2.2 W m^{-2} for fresh snow and 18.1–20.4 W m^{-2} for the dirtiest snow. Dust could reduce BC RF in snow. The BC RF on Muji Glacier exceeded those glacier snows over the TP because of BC enrichment by snowmelt.

Acknowledgments

We are grateful to Mark Flanner for guidance with SNICAR, and to two reviewers for their helpful comments which improved the manuscript. Special thanks to Silang, Tianli Xu for collecting snow samples, Suixin Liu and Zhuzi Zhao for sample analysis, and Jawad Nasir for improving the English. We also thank Guangjian Wu, Meilin Zhu, Huabiao Zhao, and Jiule Li for the guide and help in the field work. This work was partially supported by China National Funds for Distinguished Young Scholars (41125003), the Chinese Academy of Sciences (XDA05080600) and the Natural Science Foundation of China (41201058). Charles S. Zender acknowledges support from NASA (NX14AH55A).

Appendix A. Supplementary data

Supplementary data related to this article can be found at http://dx.doi.org/10.1016/j.atmosenv.2015.03.016.

References

Bond, T.C., Bergstrom, R.W., 2006. Light absorption by carbonaceous particles: an investigative review. Aerosol Sci. Tech. 40, 27–67.

Bond, T.C., Doherty, S.J., Fahey, D.W., Forster, P.M., Berntsen, T., DeAngelo, B.J., Flanner, M.G., Ghan, S., Karcher, B., Koch, D., Kinne, S., Kondo, Y., Quinn, P.K., Sarofim, M.C., Schultz, M.G., Schulz, M., Venkataraman, C., Zhang, H., Zhang, S., Bellouin, N., Guttikunda, S.K., Hopke, P.K., Jacobson, M.Z., Kaiser, J.W., Klimont, Z., Lohmann, U., Schwarz, J.P., Shindell, D., Storelvmo, T., Warren, S.G., Zender, C.S., 2013. Bounding the role of black carbon in the climate system: a scientific assessment. J. Geophys Res-Atmos. 118, 5380–5552.

Cao, J.J., Lee, S.C., Ho, K.F., Zhang, X.Y., Zou, S.C., Fung, K., Chow, J.C., Watson, J.G., 2003. Characteristics of carbonaceous aerosol in Pearl River Delta Region, China during 2001 winter period. Atmos. Environ. 37, 1451–1460.

Cao, J.J., Xu, B.Q., He, J.Q., Liu, X.Q., Han, Y.M., Wang, G.H., Zhu, C.S., 2009. Concentrations, seasonal variations, and transport of carbonaceous aerosols at a remote Mountainous region in western China. Atmos. Environ. 43, 4444–4452.

Chow, J.C., Watson, J.G., Chen, L.W.A., Arnott, W.P., Moosmuller, H., 2004. Equivalence of elemental carbon by thermal/optical reflectance and transmittance with different temperature protocols. Environ. Sci. Technol. 38, 4414–4422.

Conger, S.M., McClung, D.M., 2009. Comparison of density cutters for snow profile observations. J. Glaciol. 55, 163–169.

Conway, H., Gades, A., Raymond, C.F., 1996. Albedo of dirty snow during conditions of melt. Water Resour. Res. 32, 1713–1718.

Doherty, S.J., Grenfell, T.C., Forsstrom, S., Hegg, D.L., Brandt, R.E., Warren, S.G., 2013. Observed vertical redistribution of black carbon and other insoluble light-absorbing particles in melting snow. J. Geophys Res-Atmos. 118, 5553–5569.

Doherty, S.J., Warren, S.G., Grenfell, T.C., Clarke, A.D., Brandt, R.E., 2010. Light-absorbing impurities in Arctic snow. Atmos. Chem. Phys. 10, 11647–11680.

Flanner, M.G., Zender, C.S., 2005. Snowpack radiative heating: influence on Tibetan Plateau climate. Geophys Res. Lett. 32.

Flanner, M.G., Zender, C.S., Hess, P.G., Mahowald, N.M., Painter, T.H., Ramanathan, V., Rasch, P.J., 2009. Springtime warming and reduced snow cover from carbonaceous particles. Atmos. Chem. Phys. 9, 2481–2497.

Flanner, M.G., Zender, C.S., Randerson, J.T., Rasch, P.J., 2007. Present-day climate forcing and response from black carbon in snow. J. Geophys Res-Atmos. 112.

Forsstrom, S., Isaksson, E., Skeie, R.B., Strom, J., Pedersen, C.A., Hudson, S.R., Berntsen, T.K., Lihavainen, H., Godtliebsen, F., Gerland, S., 2013. Elemental carbon measurements in European Arctic snow packs. J. Geophys Res-Atmos. 118, 13614–13627.

Giglio, L., Csiszar, I., Justice, C.O., 2006. Global distribution and seasonality of active fires as observed with the Terra and Aqua Moderate Resolution Imaging Spectroradiometer (MODIS) sensors. J. Geophys Res-Biogeo 111.

Huang, J.P., Fu, Q.A., Zhang, W., Wang, X., Zhang, R.D., Ye, H., Warren, S.G., 2011. Dust and black carbon in seasonal snow across Northern China. B Am. Meteorol. Soc. 92, 175–181.

Kaspari, S.D., Painter, T.H., Gysel, M., Skiles, S.M., Schwikowski, M., 2014. Seasonal and elevational variations of black carbon and dust in snow and ice in the Solu-Khumbu, Nepal and estimated radiative forcings. Atmos. Chem. Phys. 14, 8089–8103.

Kaspari, S.D., Schwikowski, M., Gysel, M., Flanner, M.G., Kang, S., Hou, S., Mayewski, P.A., 2011. Recent increase in black carbon concentrations from a Mt. Everest ice core spanning 1860–2000 AD. Geophys Res. Lett. 38.

Kopacz, M., Mauzerall, D.L., Wang, J., Leibensperger, E.M., Henze, D.K., Singh, K., 2011. Origin and radiative forcing of black carbon transported to the Himalayas and Tibetan Plateau. Atmos. Chem. Phys. 11, 2837–2852.

Lee, Y.H., Lamarque, J.F., Flanner, M.G., Jiao, C., Shindell, D.T., Berntsen, T., Bisiaux, M.M., Cao, J., Collins, W.J., Curran, M., Edwards, R., Faluvegi, G., Ghan, S., Horowitz, L.W., McConnell, J.R., Ming, J., Myhre, G., Nagashima, T., Naik, V., Rumbold, S.T., Skeie, R.B., Sudo, K., Takemura, T., Thevenon, F., Xu, B., Yoon, J.H., 2013. Evaluation of preindustrial to present-day black carbon and its albedo forcing from Atmospheric Chemistry and Climate Model Intercomparison Project (ACCMIP). Atmos. Chem. Phys. 13, 2607–2634.

Michalsky, J.J., 1988. The astronomical-almanacs algorithm for approximate solar position (1950–2050). Sol. Energy 40, 227–235.

Ming, J., Cachier, H., Xiao, C., Qin, D., Kang, S., Hou, S., Xu, J., 2008. Black carbon record based on a shallow Himalayan ice core and its climatic implications. Atmos. Chem. Phys. 8, 1343–1352.

Ming, J., Xiao, C.D., Cachier, H., Qin, D.H., Qin, X., Li, Z.Q., Pu, J.C., 2009. Black carbon (BC) in the snow of glaciers in west China and its potential effects on albedos. Atmos. Res. 92, 114–123.

Ming, J., Xiao, C.D., Du, Z.C., Yang, X.G., 2013. An overview of black carbon deposition in high Asia glaciers and its impacts on radiation balance. Adv. Water Resour. 55, 80–87.

Nolin, A.W., Dozier, J., 2000. A hyperspectral method for remotely sensing the grain size of snow. Remote Sens. Environ. 74, 207–216.

Oleson, K.W., Lawrence, D.M., Bonan, G.B., Drewniak, B., Huang, M., Koven, C.D., Levis, S., Li, F., Riley, W.J., Subin, Z.M., Swenson, S.C., Thornton, P.E., Bozbiyik, A., Fisher, R., Heald, C.L., Kluzek, E., Lamarque, J., Lawrence, P.J., Leung, L.R., Lipscomb, W., Muszala, S., Ricciuto, M., Sacks, W., Sun, Y., Tang, J., Yang, Z., 2013. Technical Description of Version 4.5 of the Community Land Model (CLM), Boulder, Colorado, 80307–83000.

Painter, T.H., Skiles, S.M., Deems, J.S., Bryant, A.C., Landry, C.C., 2012. Dust radiative forcing in snow of the Upper Colorado River Basin: 1. A 6 year record of energy balance, radiation, and dust concentrations. Water Resour. Res. 48.

Qian, Y., Flanner, M.G., Leung, L.R., Wang, W., 2011. Sensitivity studies on the impacts of Tibetan Plateau snowpack pollution on the Asian hydrological cycle and monsoon climate. Atmos. Chem. Phys. 11, 1929–1948.

Ricchiazzi, P., Yang, S.R., Gautier, C., Sowle, D., 1998. SBDART: a research and teaching software tool for plane-parallel radiative transfer in the Earth's atmosphere. B Am. Meteorol. Soc. 79, 2101–2114.

Schwarz, J.P., Doherty, S.J., Li, F., Ruggiero, S.T., Tanner, C.E., Perring, A.E., Gao, R.S., Fahey, D.W., 2012. Assessing Single Particle Soot Photometer and Integrating Sphere/Integrating Sandwich spectrophotometer measurement techniques for quantifying black carbon concentration in snow. Atmos. Meas. Tech. 5, 2581–2592.

Stamnes, K., Tsay, S.C., Wiscombe, W., Jayaweera, K., 1988. Numerically stable algorithm for Discrete-Ordinate-method radiative-transfer in Multiple-scattering and Emitting layered Media. Appl. Opt. 27, 2502–2509.

Sterle, K.M., McConnell, J.R., Dozier, J., Edwards, R., Flanner, M.G., 2013. Retention and radiative forcing of black carbon in eastern Sierra Nevada snow. Cryosphere 7, 365–374.

Toon, O.B., Mckay, C.P., Ackerman, T.P., Santhanam, K., 1989. Rapid calculation of radiative heating rates and photodissociation rates in Inhomogeneous Multiple-scattering atmospheres. J. Geophys Res-Atmos. 94, 16287–16301.

Torres, A., Bond, T.C., Lehmann, C.M.B., Subramanian, R., Hadley, O.L., 2014. Measuring organic carbon and black carbon in rainwater: evaluation of methods. Aerosol Sci. Tech. 48, 239–250.

Wang, M., Xu, B.Q., Zhao, H.B., Cao, J.J., Joswiak, D., Wu, G.J., Lin, S.B., 2012. The influence of dust on quantitative measurements of black carbon in ice and snow when using a Thermal optical method. Aerosol Sci. Tech. 46, 60–69.

Wang, X., Xu, B.Q., Ming, J., 2014. An overview of the studies on black carbon and Mineral dust deposition in snow and ice cores in East Asia. J. Meteorol. Res-Prc 28, 354–370.

Warren, S.G., 2013. Can black carbon in snow be detected by remote sensing? J. Geophys Res-Atmos. 118, 779–786.

Warren, S.G., Brandt, R.E., 2008. Optical constants of ice from the ultraviolet to the microwave: a revised compilation. J. Geophys Res-Atmos. 113.

Warren, S.G., Wiscombe, W.J., 1980. A model for the spectral albedo of snow .2. Snow containing atmospheric aerosols. J. Atmos. Sci. 37, 2734–2745.

Williams, M.W., Konovalov, V.G., 2008. Central Asia Temperature and Precipitation Data, 1879–2003. USA National Snow and Ice Data Center, Boulder, Colorado.

Wiscombe, W.J., Warren, S.G., 1980. A model for the spectral albedo of snow .1. Pure snow. J. Atmos. Sci. 37, 2712–2733.

Wu, G.J., Yao, T.D., Xu, B.Q., Tian, L.D., Li, Z., Duan, K.Q., 2008. Seasonal variations of dust record in the Muztagata ice cores. Chin. Sci. Bull. 53, 2506–2512.

Xu, B.Q., Cao, J.J., Hansen, J., Yao, T.D., Joswia, D.R., Wang, N.L., Wu, G.J., Wang, M., Zhao, H.B., Yang, W., Liu, X.Q., He, J.Q., 2009a. Black soot and the survival of Tibetan glaciers. P Natl. Acad. Sci. U. S. A. 106, 22114–22118.

Xu, B.Q., Cao, J.J., Joswiak, D.R., Liu, X.Q., Zhao, H.B., He, J.Q., 2012. Post-depositional enrichment of black soot in snow-pack and accelerated melting of Tibetan glaciers. Environ. Res. Lett. 7.

Xu, B.Q., Wang, M., Joswiak, D.R., Cao, J.J., Yao, T.D., Wu, G.J., Yang, W., Zhao, H.B., 2009b. Deposition of anthropogenic aerosols in a southeastern Tibetan glacier. J. Geophys Res-Atmos. 114.

Xu, B.Q., Yao, T.D., Liu, X.Q., Wang, N.L., 2006. Elemental and organic carbon measurements with a two-step heating-gas chromatography system in snow samples from the Tibetan Plateau. Ann. Glaciol. 43, 257–262.

Yao, T.D., Thompson, L., Yang, W., Yu, W.S., Gao, Y., Guo, X.J., Yang, X.X., Duan, K.Q., Zhao, H.B., Xu, B.Q., Pu, J.C., Lu, A.X., Xiang, Y., Kattel, D.B., Joswiak, D., 2012. Different glacier status with atmospheric circulations in Tibetan Plateau and surroundings. Nat. Clim. Change 2, 663–667.